

S1 Additional figures

S1.1 Significance testing

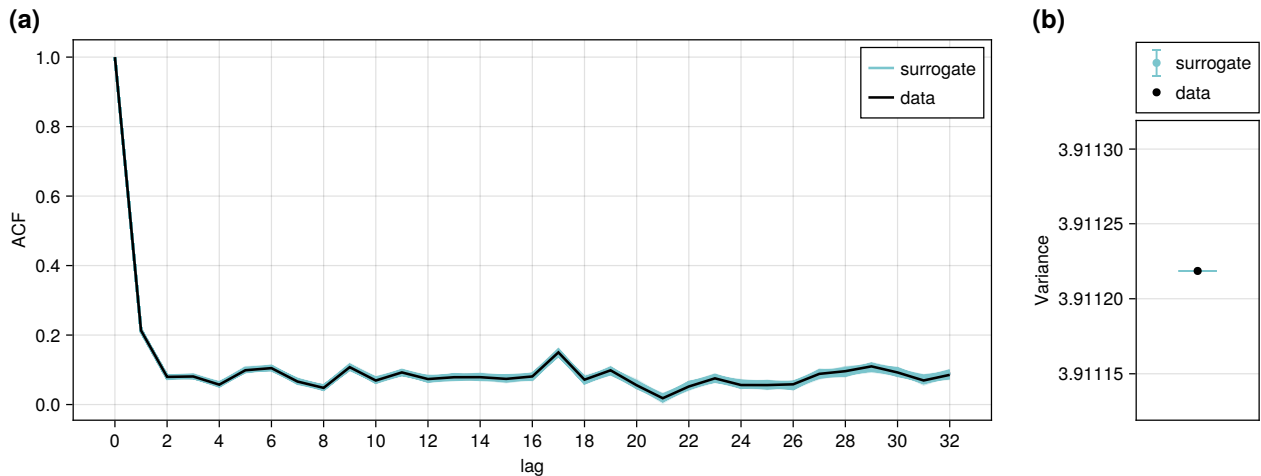


Figure S1. Autocorrelation function (a) and variance (b) of the NGRIP $\delta^{18}\text{O}$ record in 5-year resolution (black) and its TFTS surrogates (blue) during the longest GS considered prior to DO-1.

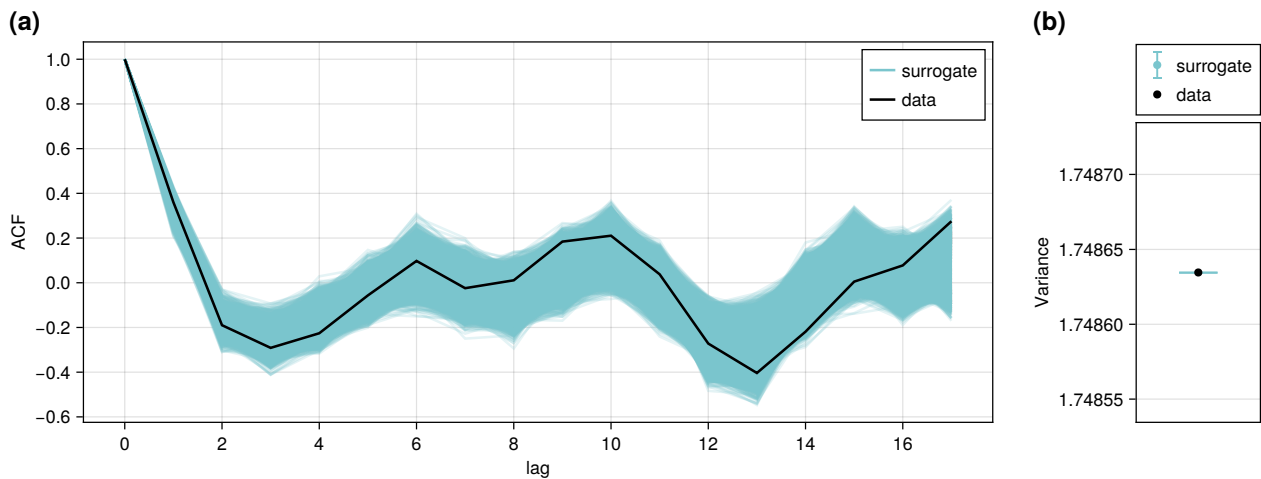
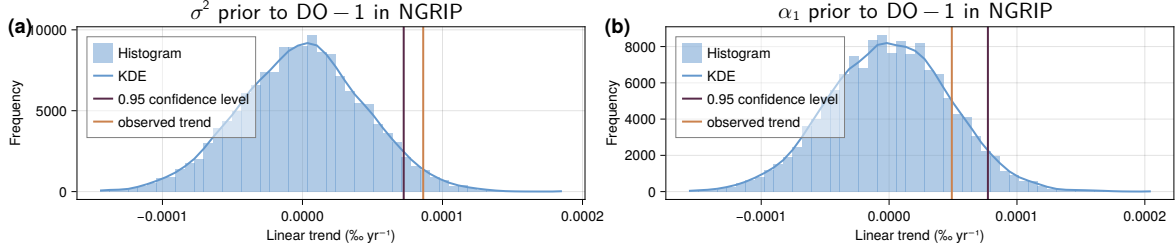
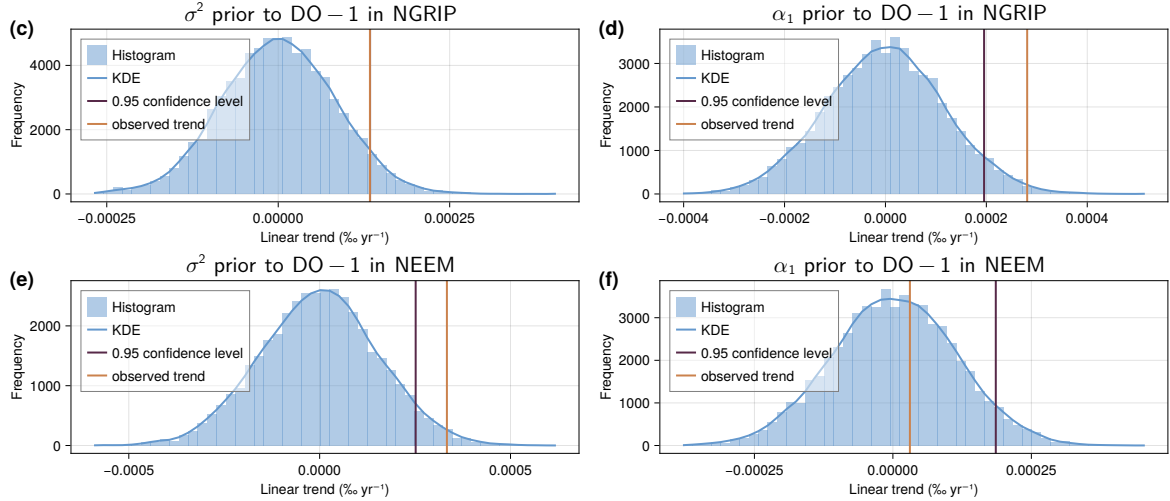


Figure S2. Autocorrelation function (a) and variance (b) of the NGRIP $\delta^{18}\text{O}$ record in 5-year resolution (black) and its TFTS surrogates (blue) during the shortest GS considered prior to DO-16.

Null-model distribution of linear trends in EWS of 100-year high-pass filtered records with 5-year resolution



Null-model distribution of linear trends in EWS of 100-year high-pass filtered records with 10-year resolution



Null-model distribution of linear trends in EWS of 100-year high-pass filtered records with 20-year resolution

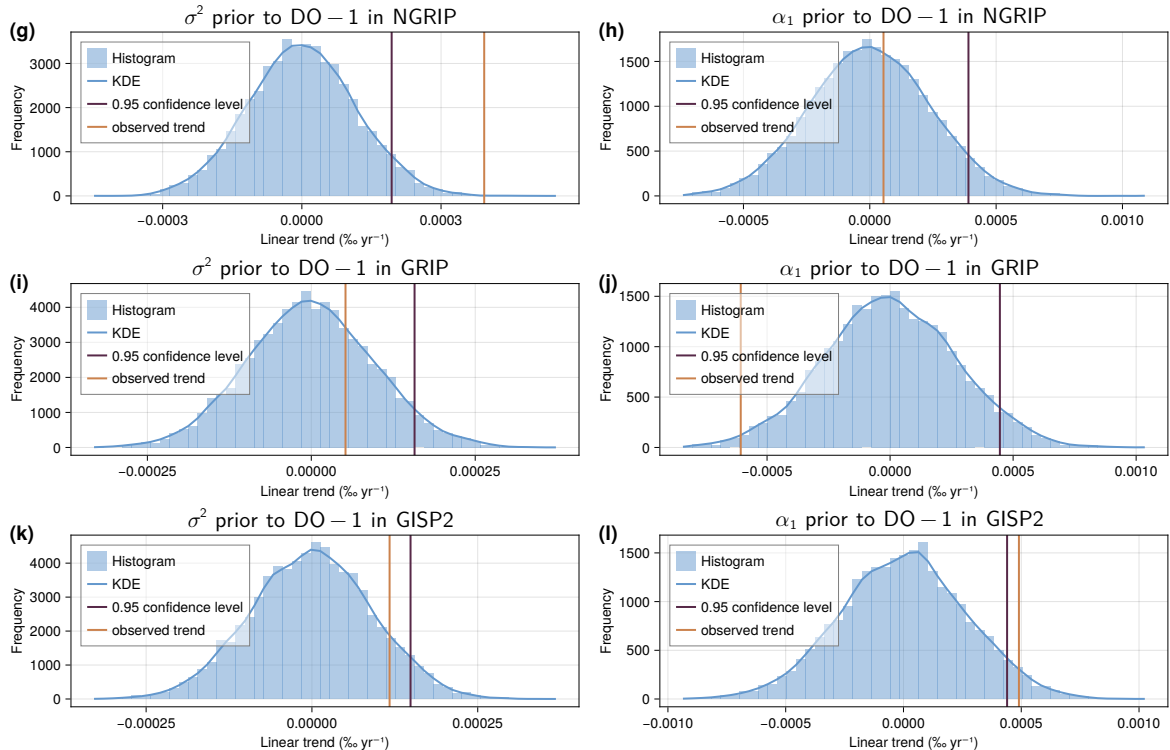
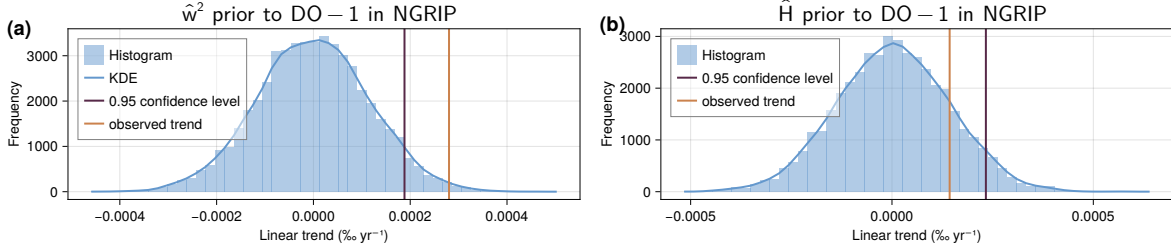
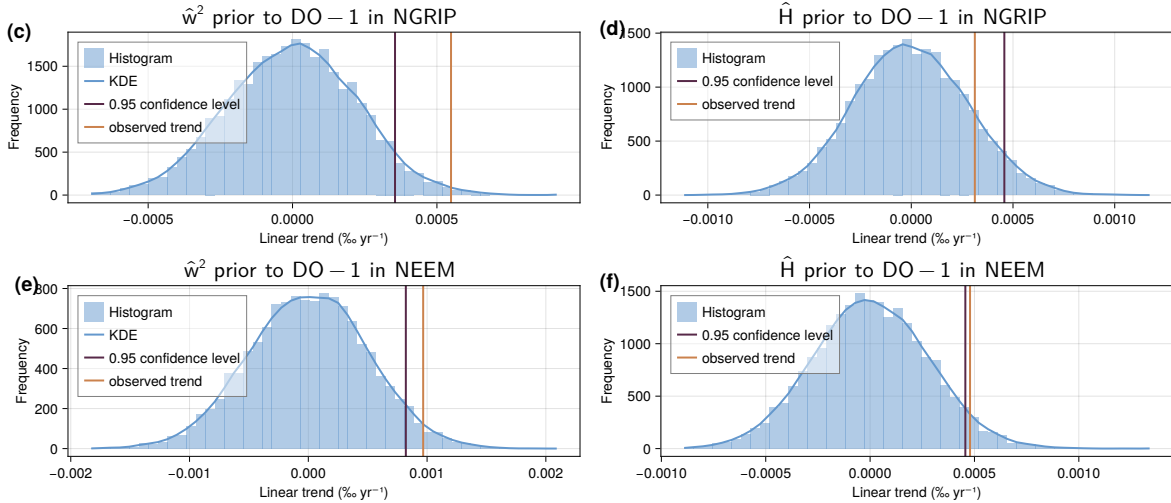


Figure S3. Null-model distribution for linear trends in the CSD-based EWS estimators prior to DO-1 in the NGRIP record in 5- (a,b), 10- (c,d) and 20-year resolution (g,h), NEEM (e,f), GRIP (i,j), and GISP2 (k,l). Those for the variance are shown in the left column (a,c,e,g,i,k), those for the lag-1 autocorrelation coefficient in the right (b,d,f,h,j,l). Histograms, kernel density estimates of the probability density function, and confidence levels of the null-model distributions are obtained from 10 000 surrogates with partially randomised phases of the records in the GS prior to DO-1 (see main text Sect. 2.3).

Null-model distribution of linear trends in EWS of (20-60) year band of records with 5-year resolution



Null-model distribution of linear trends in EWS of (20-60) year band of records with 10-year resolution



Null-model distribution of linear trends in EWS of (20-60) year band of records with 20-year resolution

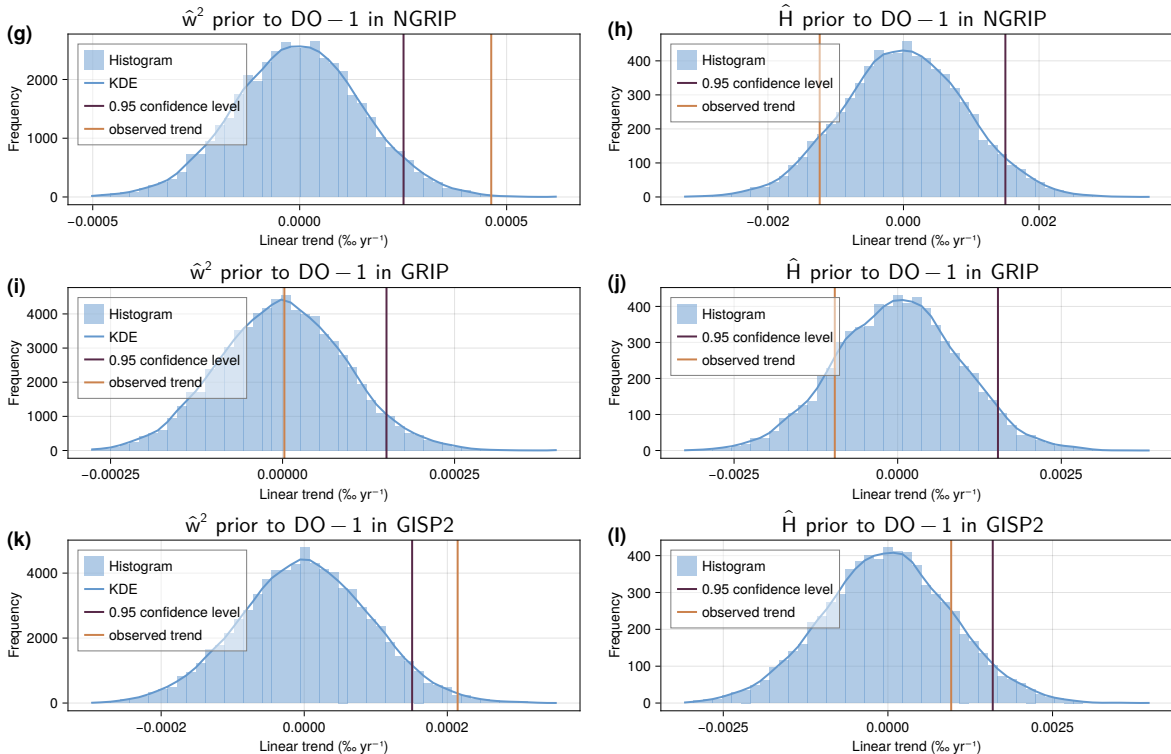


Figure S4. Null-model distribution for linear trends in the wavelet-based EWS estimators prior to DO-1 in the NGRIP record in 5- (a,b), 10- (c,d) and 20-year resolution (g,h), NEEM (e,f), GRIP (i,j), and GISP2 (k,l). Those for the scale-averaged wavelet coefficient are shown in the left column (a,c,e,g,i,k), those for the local Hurst exponent in the right (b,d,f,h,j,l). Histograms, kernel density estimates of the probability density function, and confidence levels of the null-model distributions are obtained from 10 000 surrogates with partially randomised phases of the records in the GS prior to DO-1 (see main text Sect. 2.3).

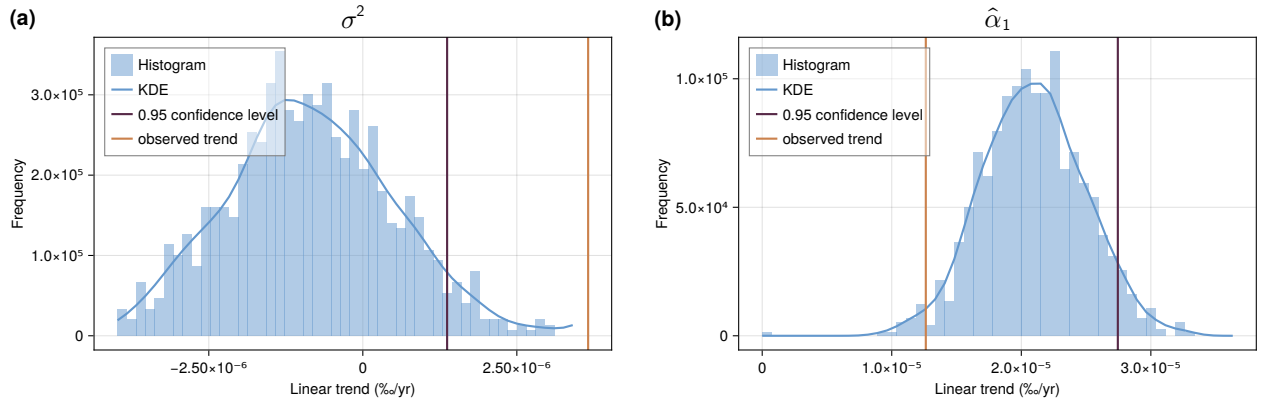


Figure S5. Null-model distribution for linear trends in the CSD-based EWS estimators variance (a) and autocorrelation (b) prior to DO-1 in the raw NGRIP record with irregular time steps. Histograms, kernel density estimates of the probability density function, and confidence levels of the null-model distributions are obtained from 1 000 surrogates with partially randomised phases of the record in the GS prior to DO-1 (see main text Sect. 2.3).

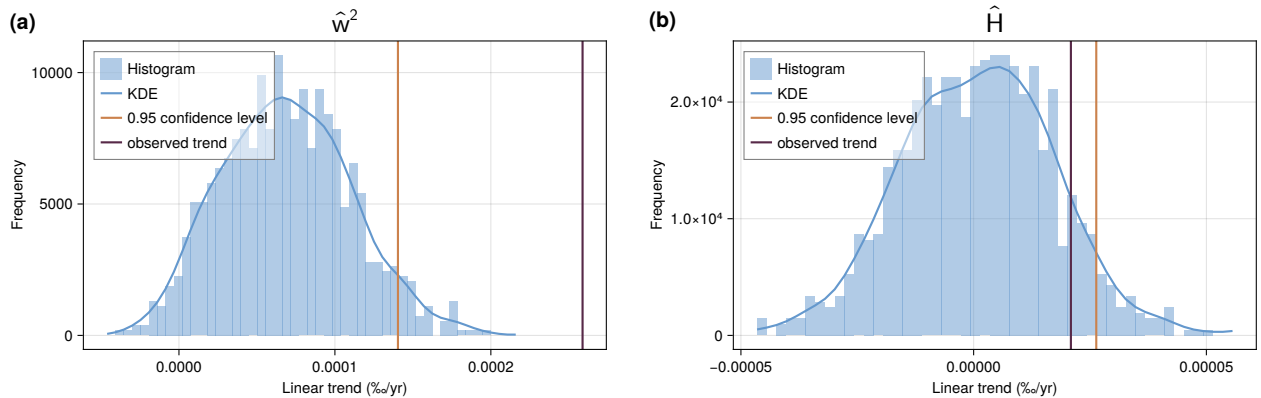


Figure S6. Null-model distribution for linear trends in the wavelet-based EWS estimators scale-averaged wavelet coefficient (a) and local Hurst exponent (b) prior to DO-1 in the raw NGRIP record with irregular time steps. Histograms, kernel density estimates of the probability density function, and confidence levels of the null-model distributions are obtained from 1 000 surrogates with partially randomised phases of the record in the GS prior to DO-1 (see main text Sect. 2.3).

S1.2 CSD-based EWS

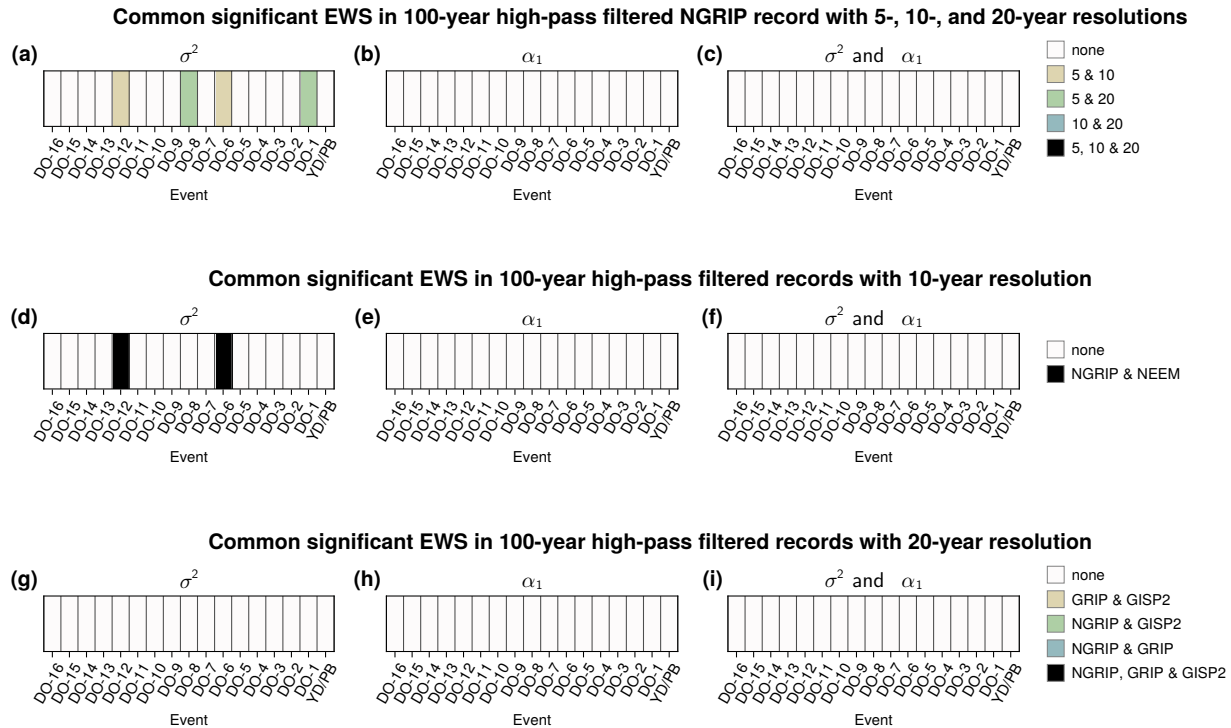


Figure S7. Common significant EWS in the CSD indicators for individual transitions across the $\delta^{18}\text{O}$ NGRIP record with different temporal resolutions (a-c), records with 10- (d-f) and 20-year resolution (g-i). Common significant increases of the variance are shown in the left (a,d,e), those of the lag-1 autocorrelation coefficient in the middle column (b,e,h). The right column shows those simultaneously occurring in both CSD estimators.

S1.3 Wavelet-based EWS

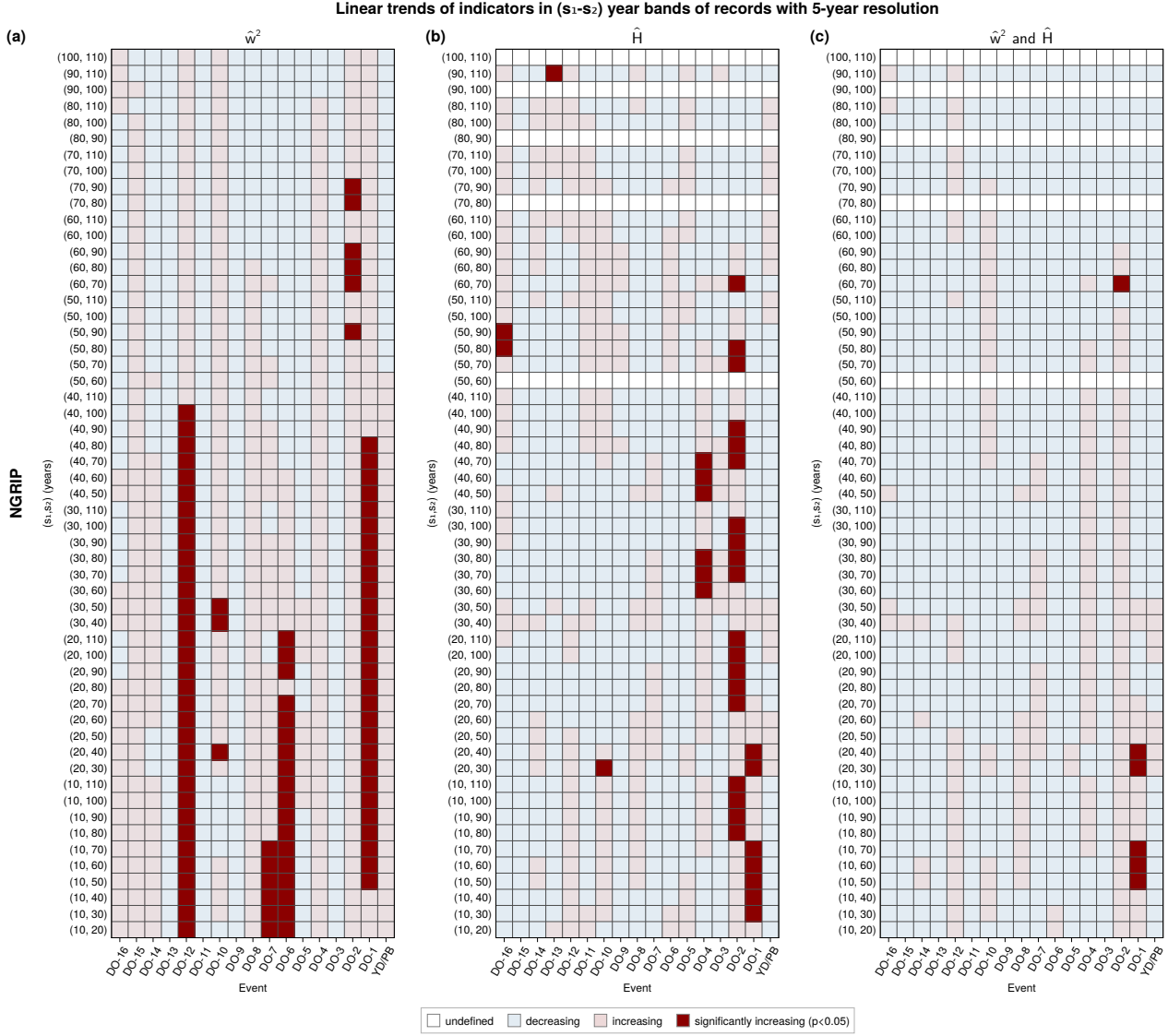


Figure S8. Same as Fig. A4 (a-c) in the main text, but including all scale ranges (s_1, s_2) considered for the NGRIP record with 5-year resolution.

Linear trends of indicators in (s_1, s_2) year bands of records with 10-year resolution

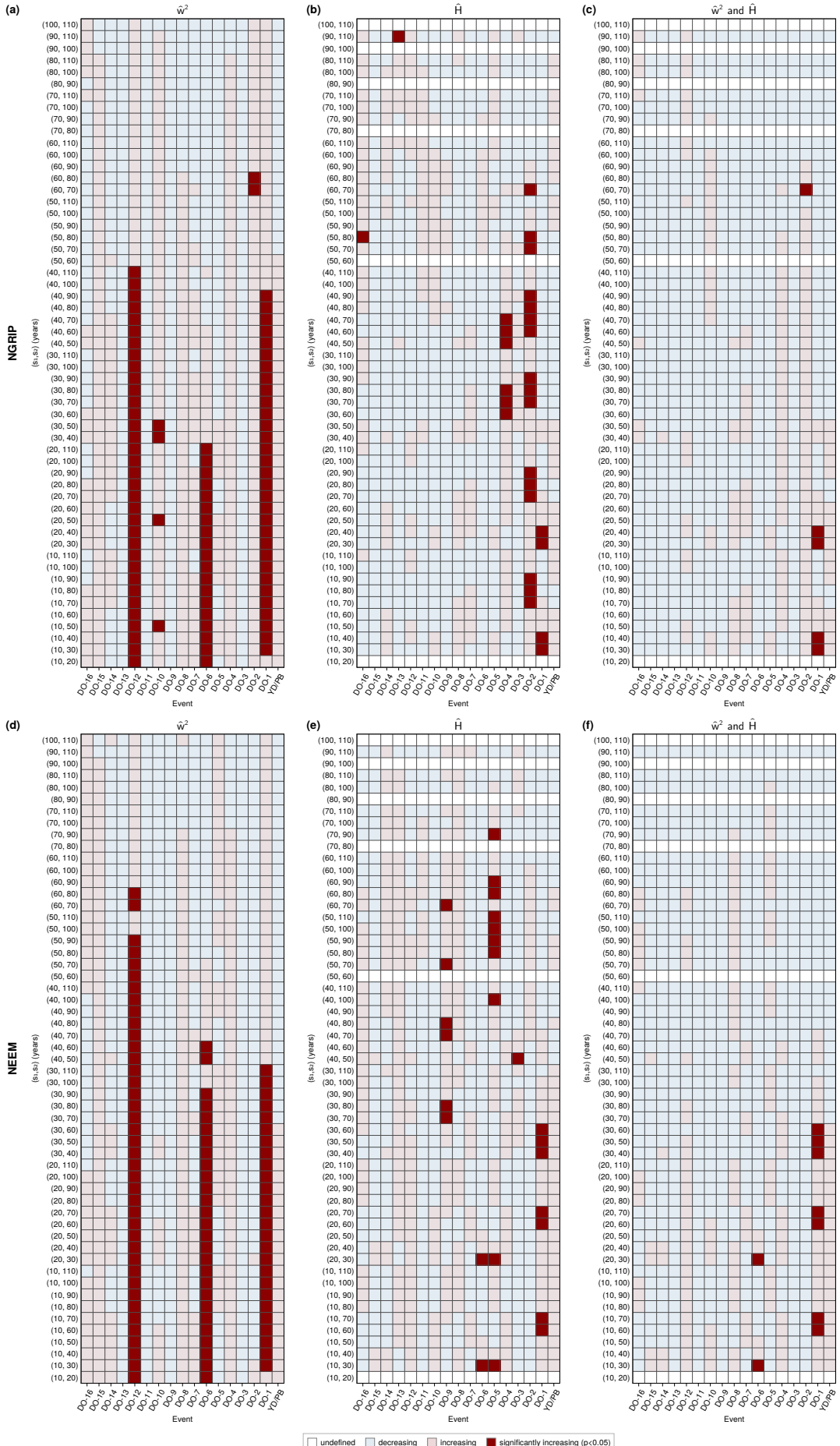


Figure S9. Same as Fig. A4 (d-i) in the main text, but including all scale ranges (s_1, s_2) considered for the NGRIP and NEEM records with 10-year resolution.

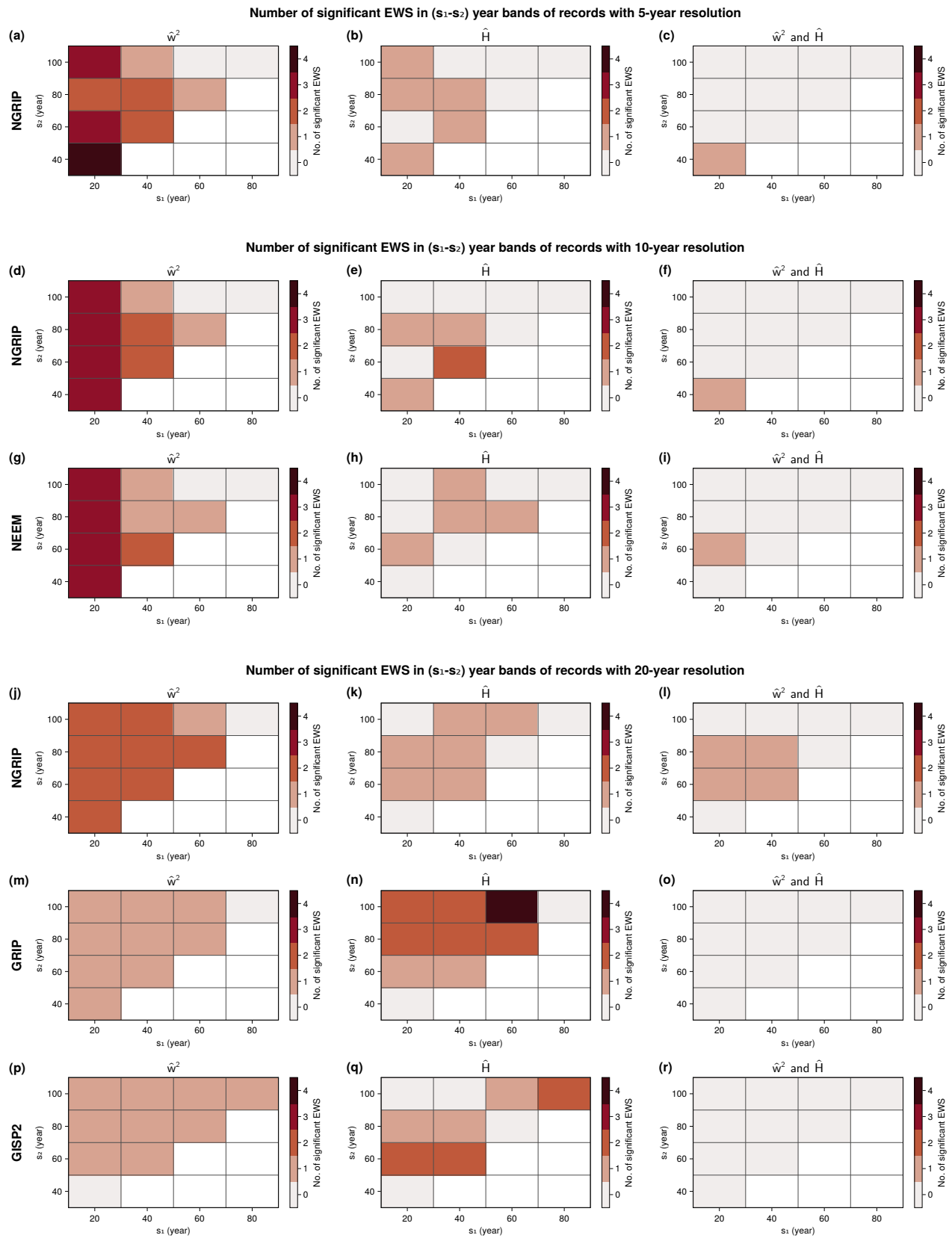
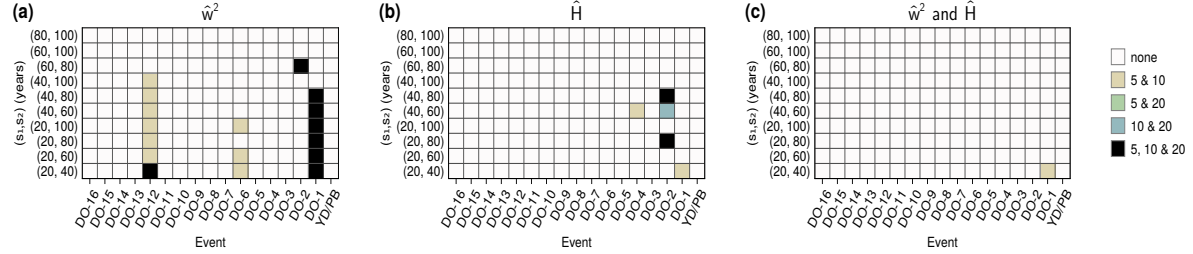
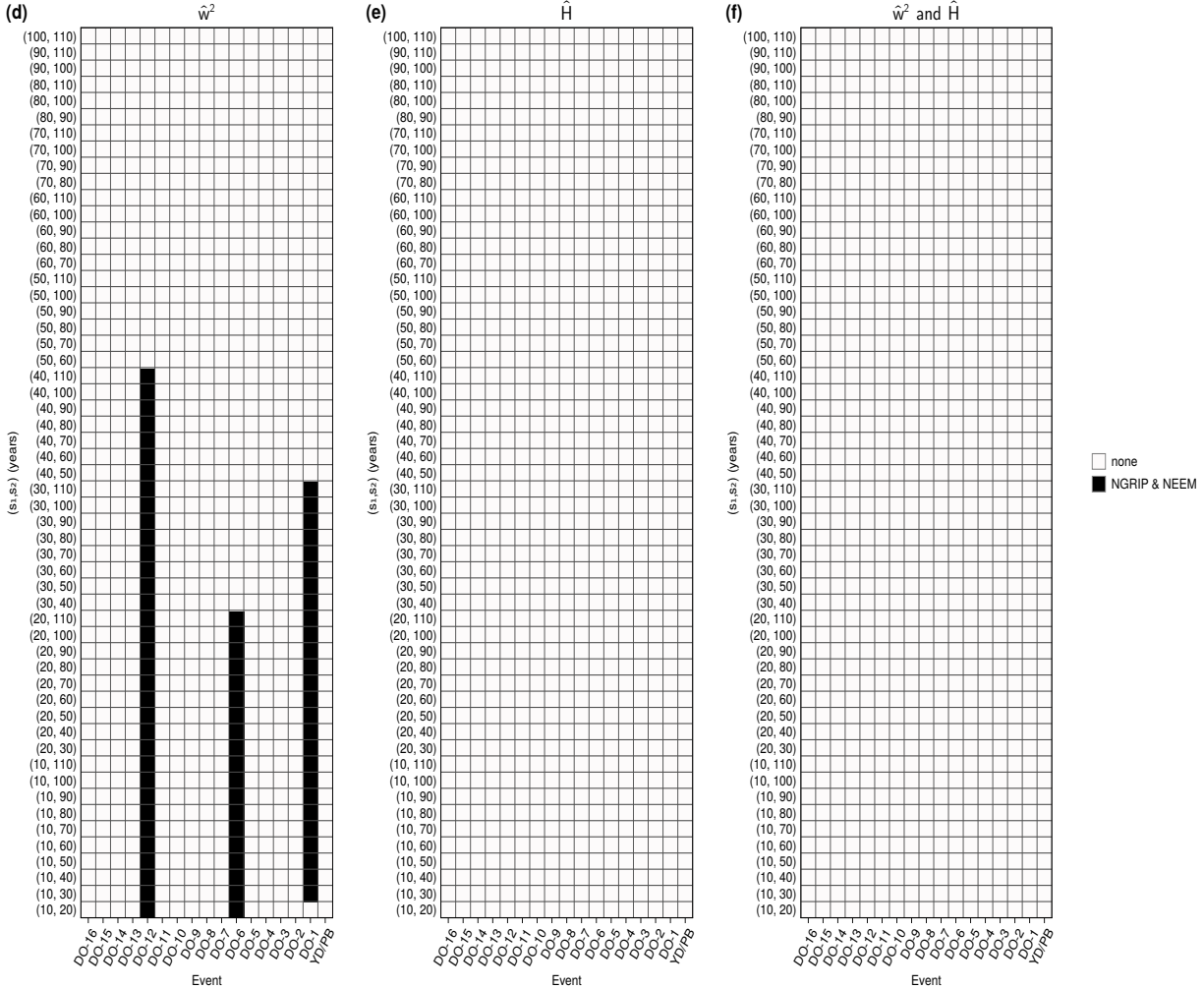


Figure S10. Same as Fig. A5 in the main text, but only including scale ranges (s_1, s_2) applicable to all $\delta^{18}\text{O}$ records with different temporal resolutions.

Common significant EWS in in (s_1-s_2) year bands of the NGRIP record with 5-, 10-, and 20-year resolutions



Common significant EWS in in (s_1-s_2) year bands of records with 10-year resolution



Common significant EWS in in (s_1-s_2) year bands of records with 20-year resolution

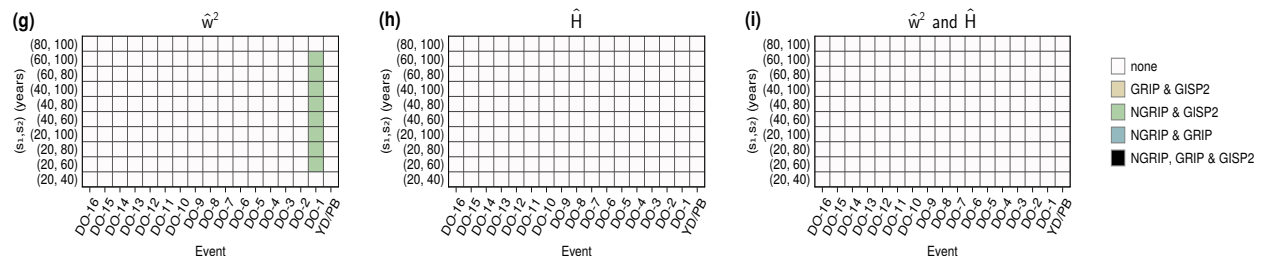


Figure S11. Common significant EWS in the wavelet-based indicators for individual transitions and various scale ranges (s_1, s_2) across the $\delta^{18}\text{O}$ NGRIP record with different temporal resolutions (a-c), records with 10- (d-f) and 20-year resolution (g-i). Common significant increases of the scale-averaged wavelet coefficient are shown in the left (a,d,e), those of the local Hurst exponent in the middle column (b,e,h). The right column shows those simultaneously occurring in both estimators.

S1.4 Detailed method comparison for NGRIP in 5-year resolution

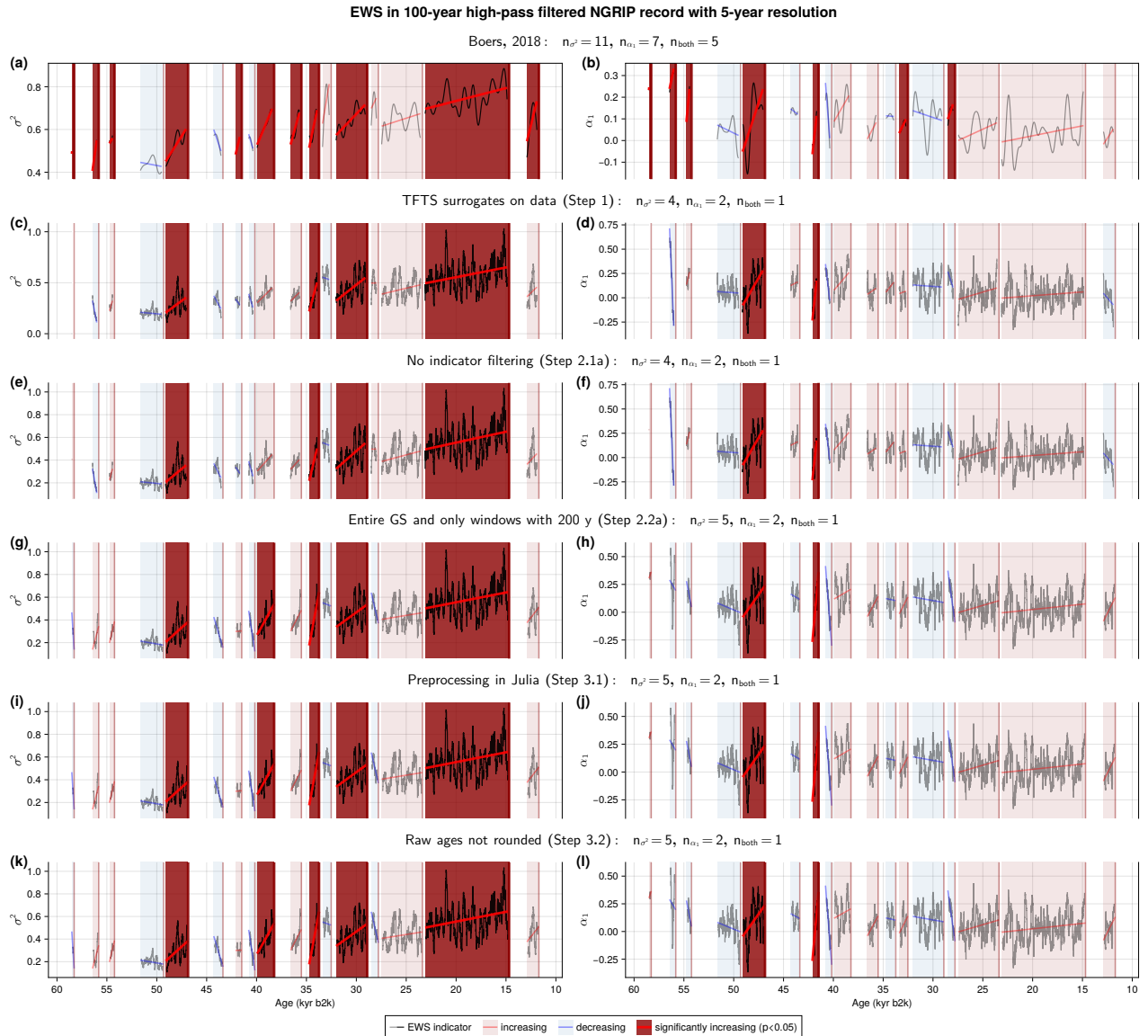


Figure S12. Same as Fig. 4 in the main text, but including the sub-steps described in Table 1 for sequential modifications to significance testing (c,d), CSD-based EWS calculation (e-h), and data preprocessing (i-l).

EWS in (10-50) year band of NGRIP record with 5-year resolution

Boers, 2018: $n_{\text{w}} = 12$, $n_{\text{H}} = 8$, $n_{\text{both}} = 7$

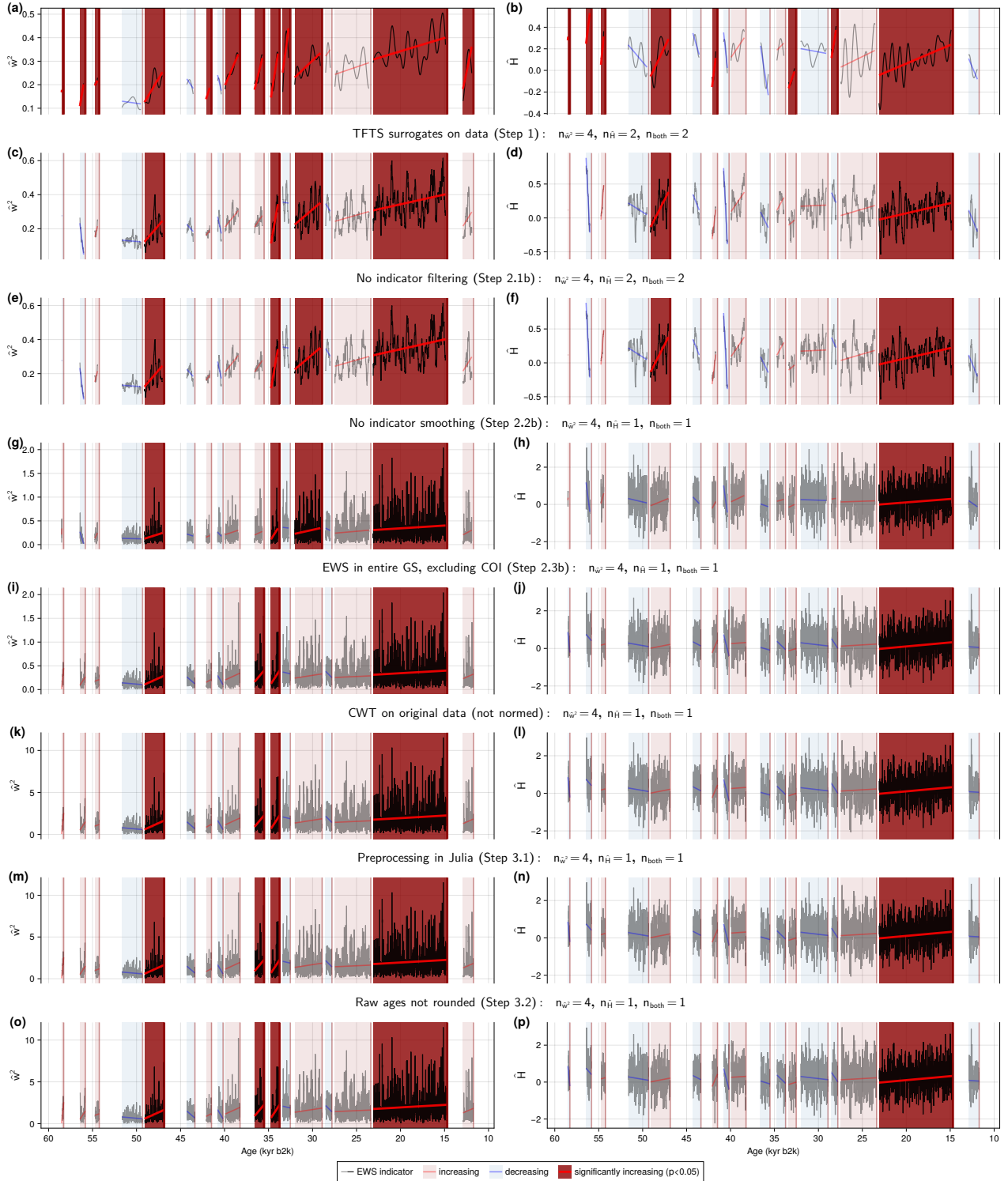


Figure S13. Same as Fig. 7 in the main text, but including the sub-steps described in Table 1 for sequential modifications to significance testing (c,d), wavelet-based EWS calculation (e-l), and data preprocessing (m-p).

S2 Results without low-pass filtering during interpolation

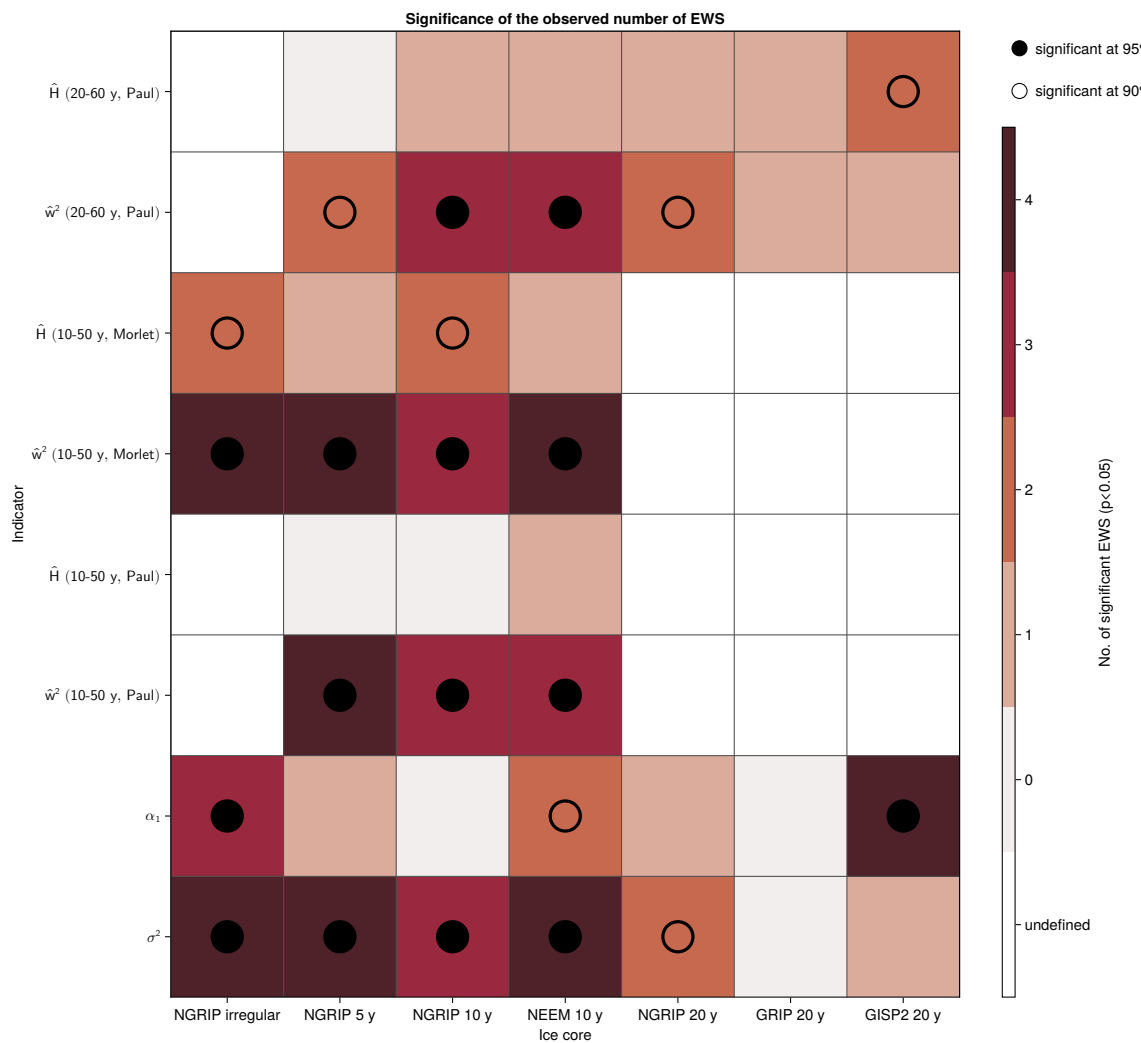


Figure S14. Same as Fig. 10 in the main text, but including the records in 5- and 10-year temporal resolution, where no low-pass filter has been applied between interpolation of the irregularly sampled record and resampling.

S2.1 CSD-based EWS

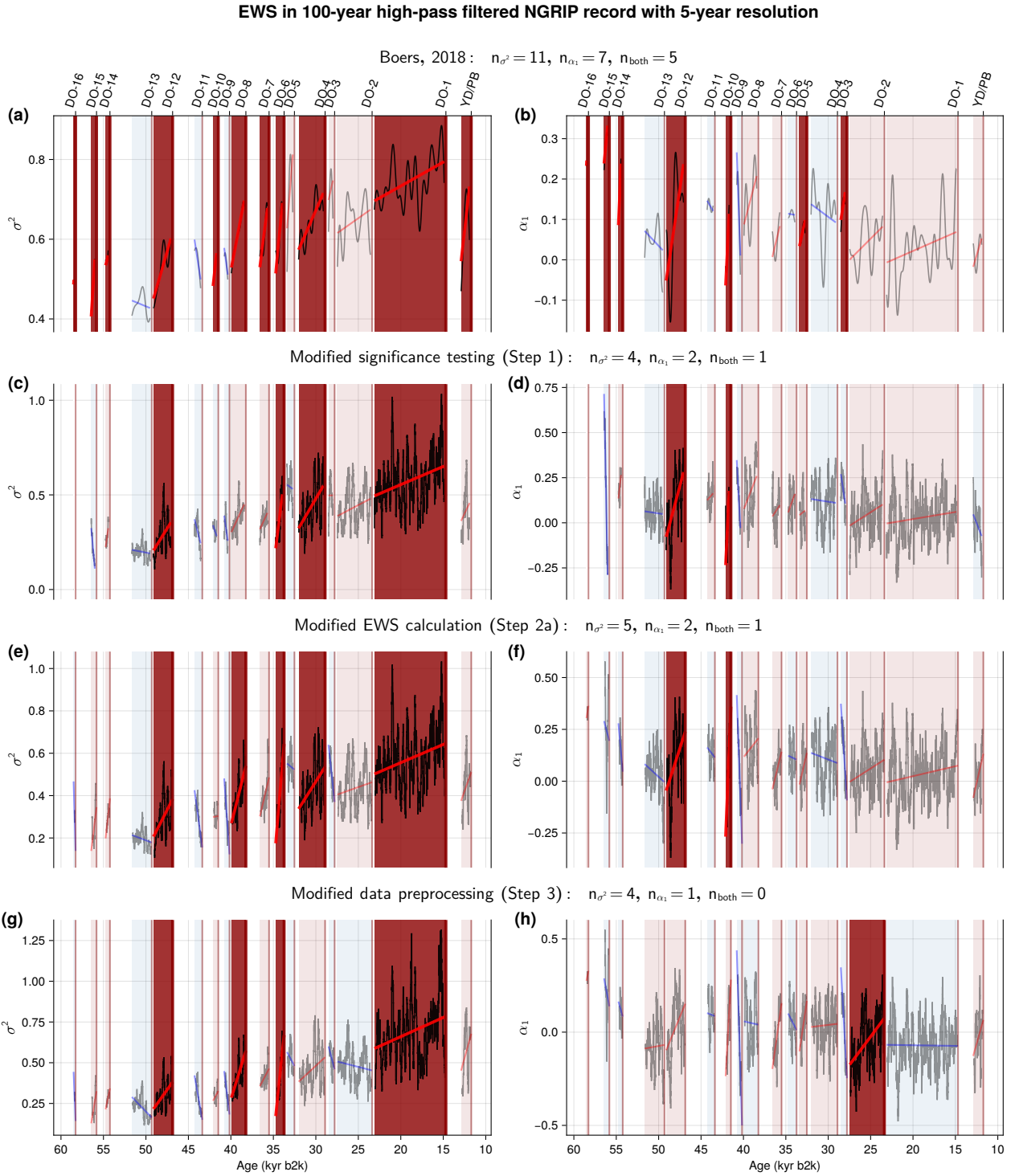


Figure S15. Same as Fig. 4 in the main text, but for the NGRIP record in 5-year temporal resolution, where no low-pass filter has been applied between interpolation of the irregularly sampled record and resampling.

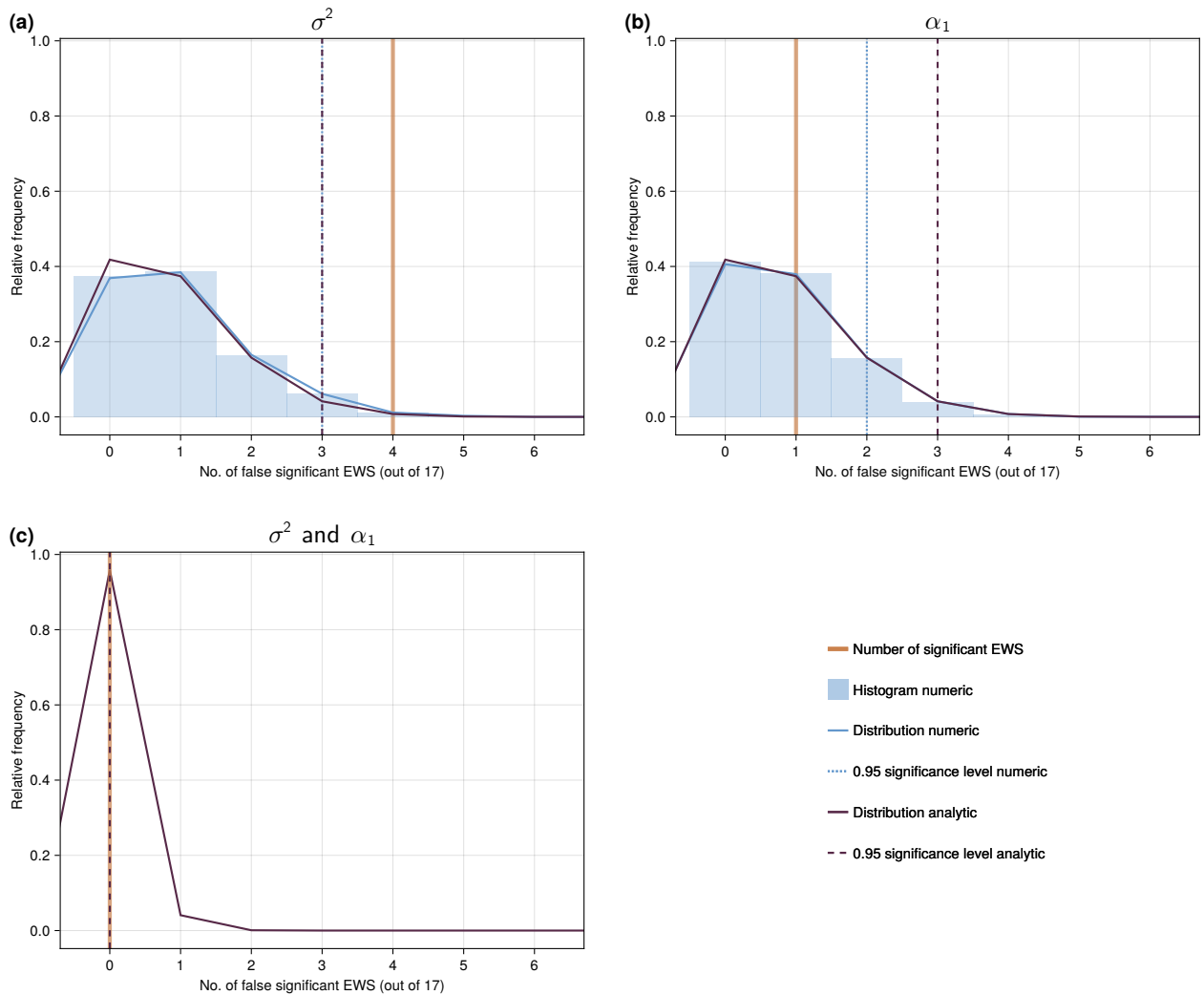


Figure S16. Same as Fig. 3 in the main text, but for the NGRIP record with 5-year temporal resolution, where no low-pass filter has been applied between interpolation of the irregularly sampled record and resampling.

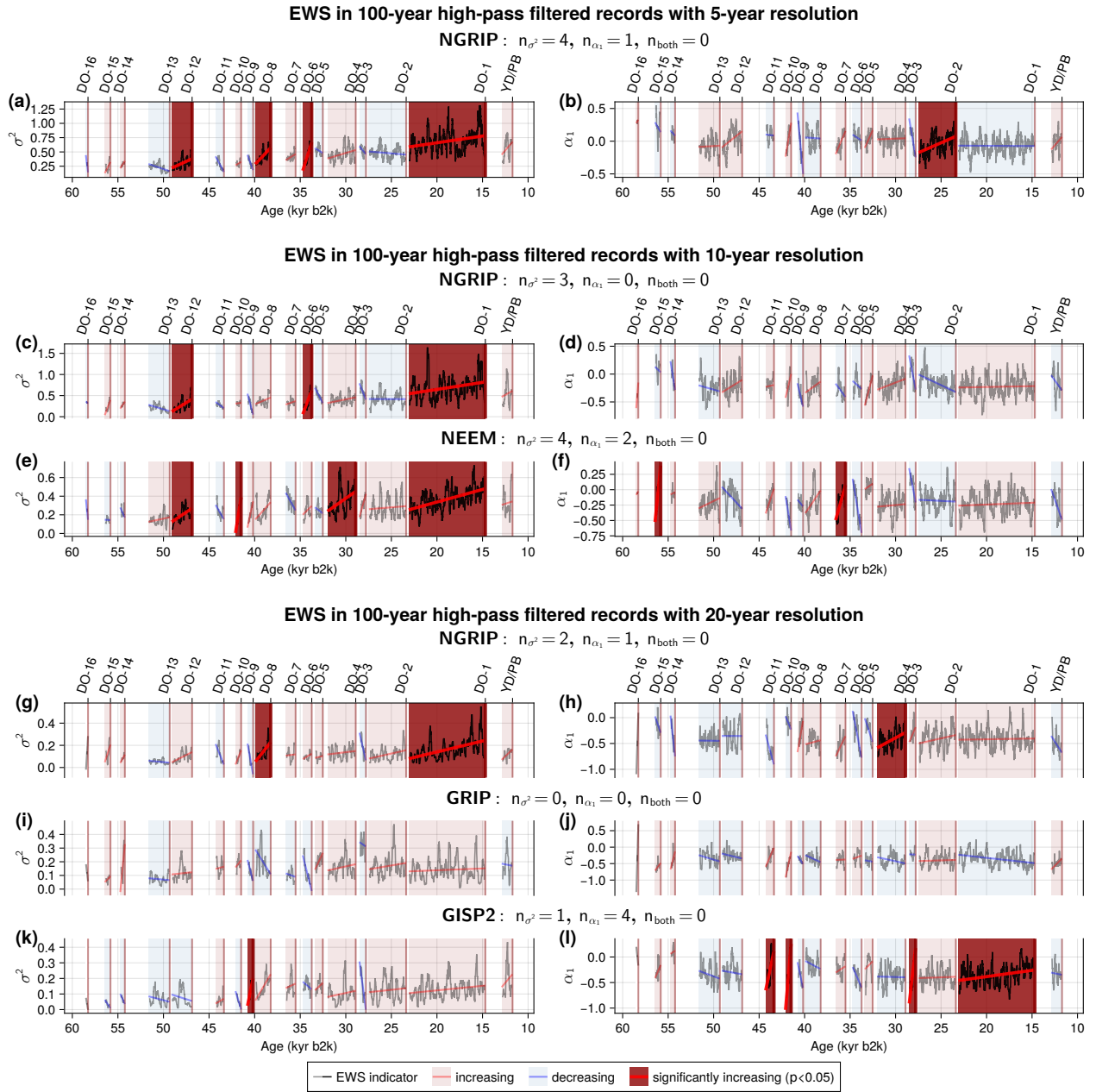


Figure S17. Same as Fig. 6 in the main text, but including the records in 5- (a,b) and 10-year temporal resolution (c-f), where no low-pass filter has been applied between interpolation of the irregularly sampled record and resampling.

S2.2 Wavelet-based EWS

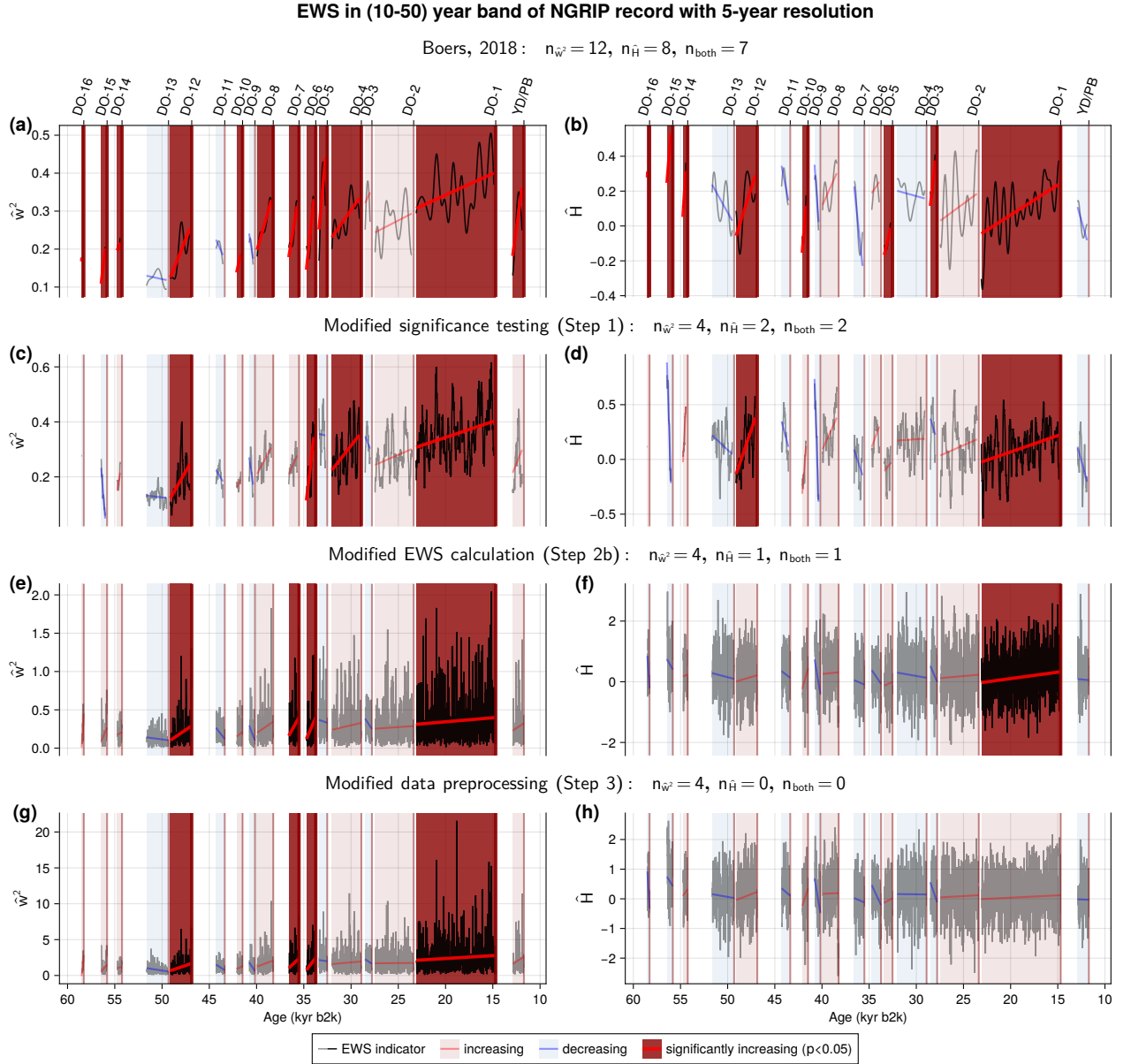


Figure S18. Same as Fig. 7 in the main text, but for the NGRIP record in 5-year temporal resolution, where no low-pass filter has been applied between interpolation of the irregularly sampled record and resampling.

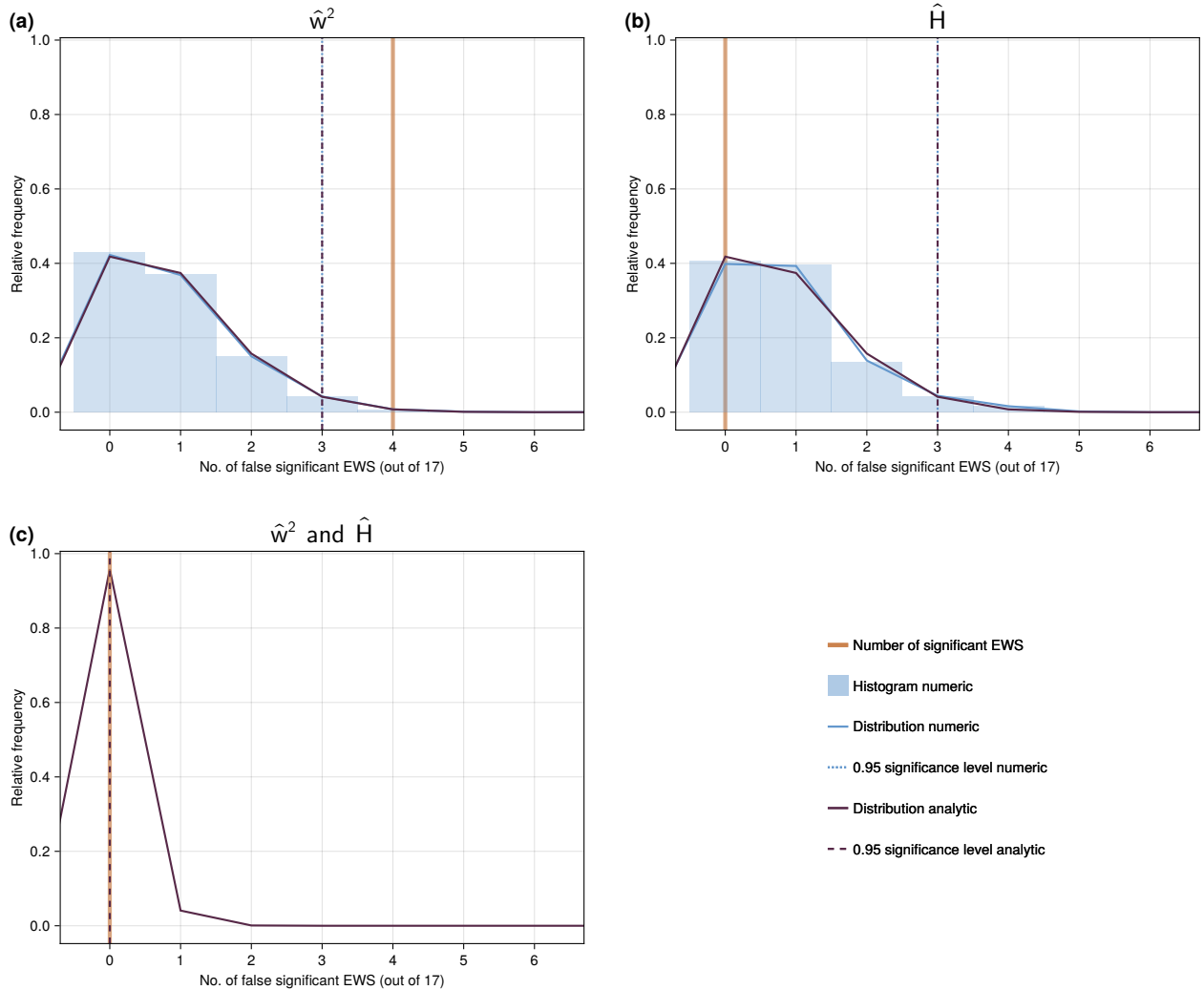


Figure S19. Same as Fig. A3 in the main text, but for the NGRIP record with 5-year temporal resolution, where no low-pass filter has been applied between interpolation of the irregularly sampled record and resampling.

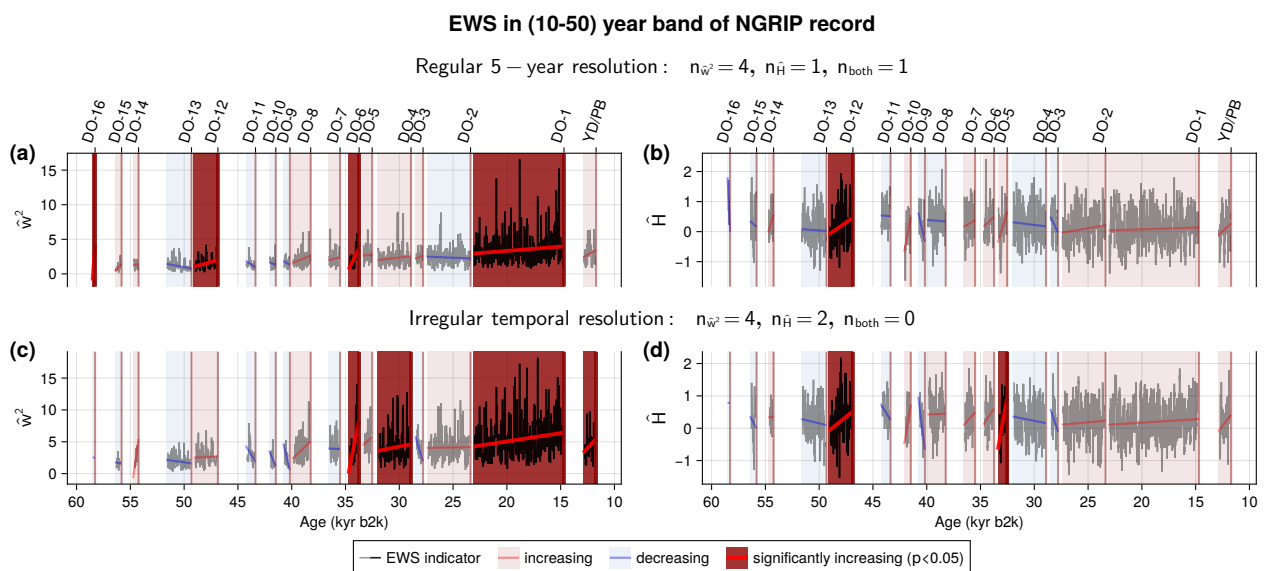


Figure S20. Same as Fig. 8 in the main text, but including the NGRIP record in 5-year resolution (a,b), where no low-pass filter has been applied between interpolation of the irregularly sampled record and resampling.

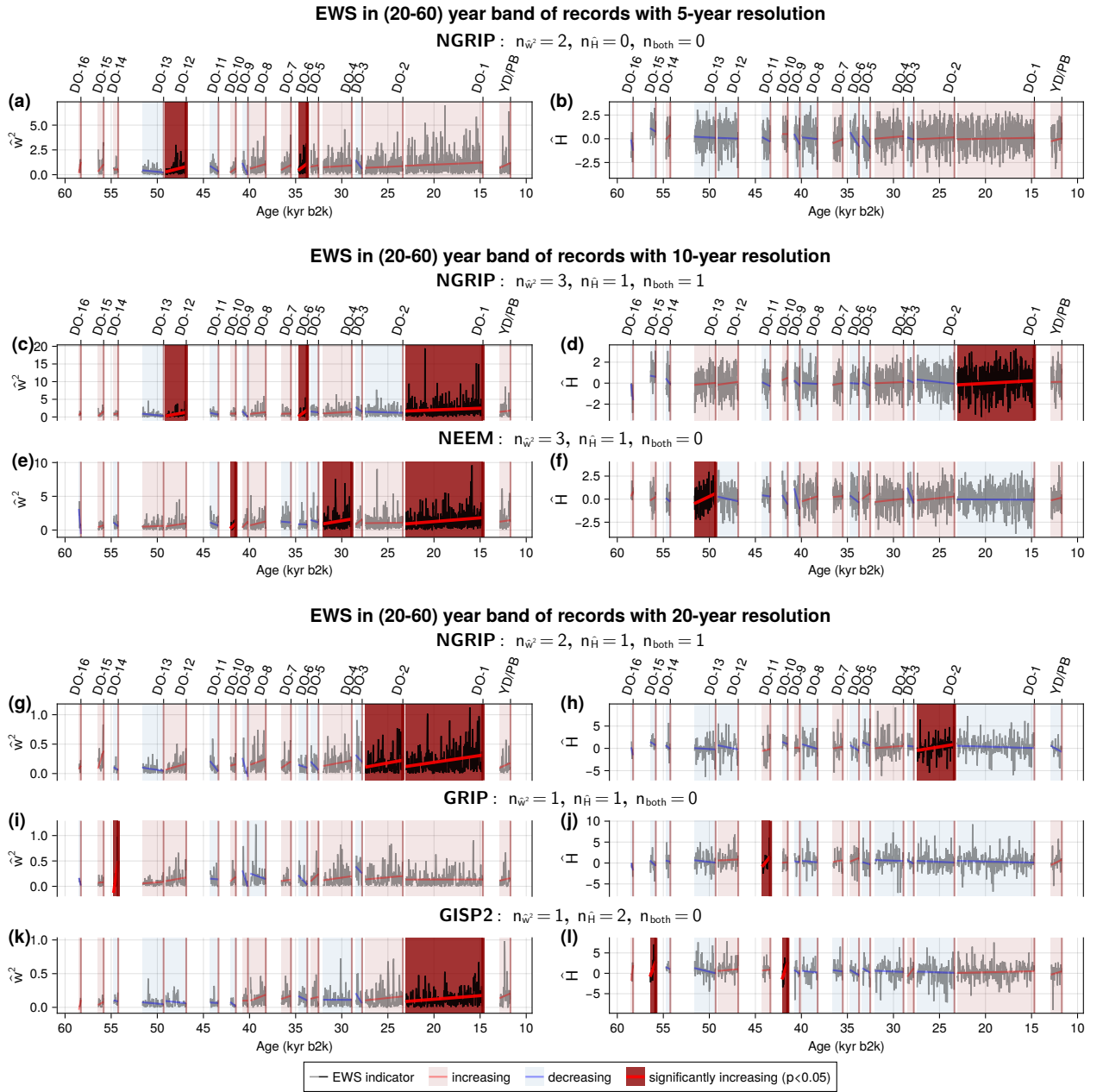
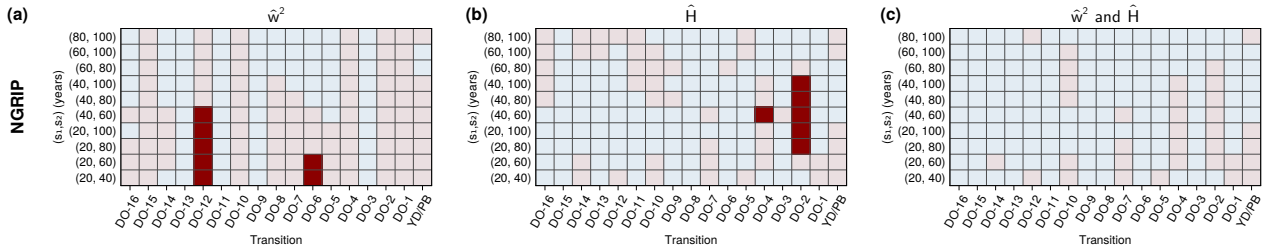
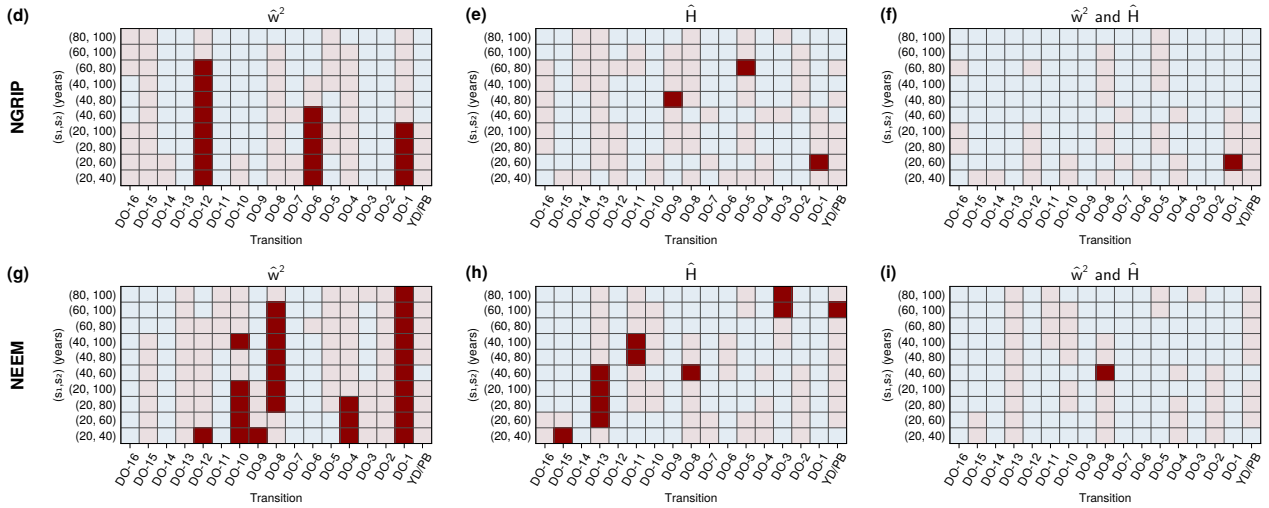


Figure S21. Same as Fig. 9 in the main text, but including the records in 5- (a,b) and 10-year temporal resolution (c-f), where no low-pass filter has been applied between interpolation of the irregularly sampled record and resampling.

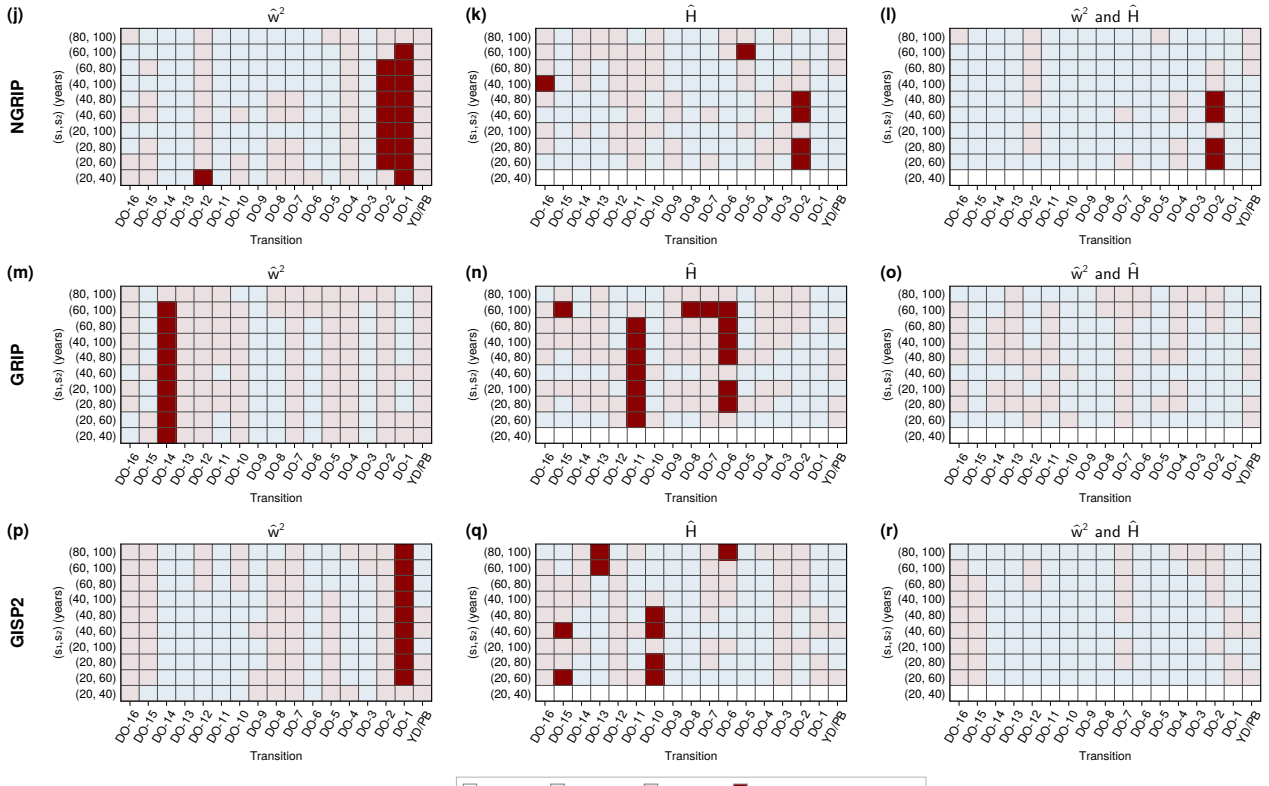
Linear trends of indicators in (s_1-s_2) year bands of records with 5-year resolution



Linear trends of indicators in (s_1-s_2) year bands of records with 10-year resolution



Linear trends of indicators in (s_1-s_2) year bands of records with 20-year resolution



Legend: □ undefined ■ decreasing ■ increasing ■ significantly increasing ($p < 0.05$)

Figure S22. Same as Fig. A4 in the main text, but including the records in 5- (a,c) and 10-year temporal resolution (d-i), where no low-pass filter has been applied between interpolation of the irregularly sampled record and resampling.

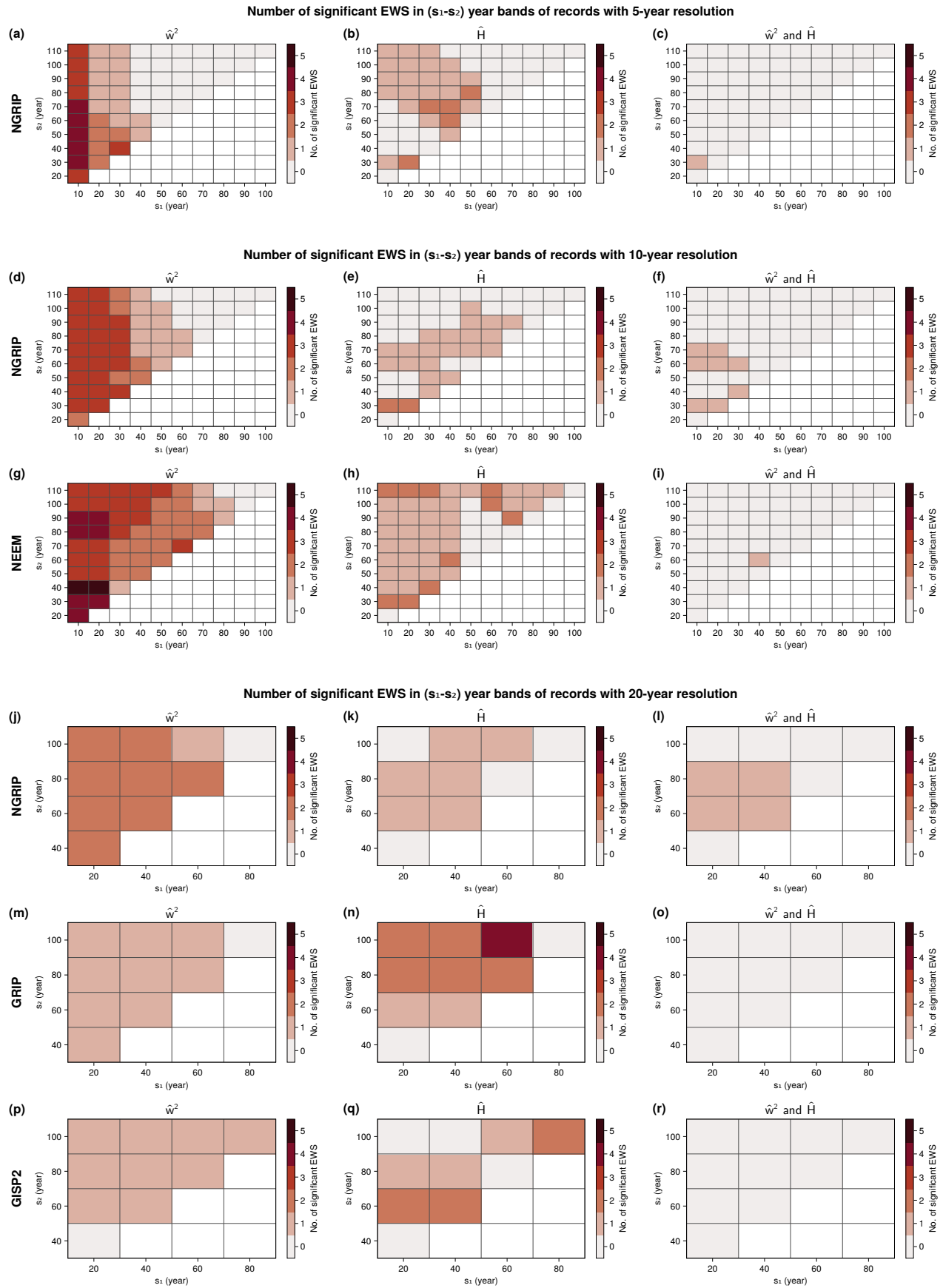


Figure S23. Same as Fig. A5 in the main text, but including the records in 5- (a,c) and 10-year temporal resolution (d-i), where no low-pass filter has been applied between interpolation of the irregularly sampled record and resampling.